Pramana–J. Phys. (#) #: ####
DOI #/#

Enhancement of fusion energy gain due to the injection of solid boron to fuel capsule utilizing the deuteron beam radiation

REZA KHORRAMDEL[1], SEYEDEH NASRIN HOSSEINI MOTLAGH[1,*] and ZOHREH PARANG[1]

[1] Department of Physics, Shiraz Branch, Islamic Azad University, Shiraz, Iran

[*]Corresponding author. E-mail: nasrinhosseinimotlagh@gmail.com

MS received 1 January 2023; revised 1 January 2023; accepted 1 January 2023

Abstract. In a tritium generator D-T reactor, large amounts of neutrons are produced. Although a ^{3}He fusion reactor produces fewer neutrons, ^{3}He resources are also scarce on Earth. Due to a large amount of available deuterium fuel sources, a D-D reactor on Earth is an ideal reactor, although it also produces tritium and ns, but their production rate is not so high. In this paper, the temperature and time behavior of an ArF laser driven fusion reactor containing a functional D-D fuel in the low temperature region controlled through the injection of a solid ^{11}B capsule is investigated for the first time, whose main fuel is deuterium and boron is the additional fuel. To increase its energy gain, we use the fast ignition of the cone guided. The results of our calculations show that the injection of deuteron beam simultaneously with laser beam irradiation to the desired spherical fuel capsule causes the bonus energy to be deposited in the fuel capsule and the energy gain increases depending on the amount of deuteron beam energy, and along with that injection of solid boron into D-D fuel increases the energy gain at 100 keV about 10 times.

Keywords. boron, deuterium, gain, laser fusion, temperature, time

PACS Nos

1. Introduction

In the past few decades, the use of energy from nuclear fusion with the inertial confinement method has received much attention, and different plans have been presented in this regard. The main goal of these plans is to achieve high energy gain [1, 2, 3]. Considering the problems in conventional fusion methods, another method in which called "fast ignition" has been proposed to reduce hydrodynamic instabilities and obtain high energy gain [4, 5].In this method, unlike the central hot spot ignition method, the heating and ignition processes are separated to reduce the required energy and as a result, reduce instabilities and achieve higher energy gain [6].In the main idea, the relativistic electron beam is used as the most suitable source for hot spot ignition. Studies on the possibility of fast ignition with relativistic electrons have been conducted in many laboratories. This method has the problem of depositing energy and focusing [7]. The use of ion beams has advantages such as classical interaction with fuel, relatively low ignition energy compared to electrons, better energy release, improved beam focusing, straight trajectory, maximum energy release at the end of their range (Bragg peak), and presentation of all kinds of instabilities [8].

Fast ignition using p beams has been suggested due to the wide energy range of p sources created by laser, significant power increase in dense fuel, solving the problem of focusing and transmission [9]. But currently, laser-to-ion converter plates that are used to produce p ions, can create p beam fluxes several orders of magnitude lower than the total fluxes required for practical fast ignition.

Carbon ion beams are proposed as another option for using in fast ignition because they are better focused on the center of the compressed fuel capsule and require fewer ion currents. But it should be noted that laser intensities much higher than what will be available in the near future are needed for their production [10]. Today, it is possible to use the innovative design of deuteron beams, which, in addition to heat transfer, causes fueling in fusion reactors by the inertial confinement method [11, 12].

On the other hand, their stopping power in fuel is more than electrons, and they can create a higher energy density due to stopping in a smaller volume of fuel. Therefore, creating additional fusion energy gain with them is a unique feature that can be used to reduce the total required deuteron flux. Alternately, it will reduce the energy of the required incident laser beam, which can play a significant role in increasing the efficiency of commercial fusion reactors. In a tritium generator D-T reactor, large amounts of ns are produced. Although a D$-^3$He fusion reactor produces fewer ns, but the resources of ^{3}He are also scarce on Earth. Due to a large amount of available deuterium fuel sources, a D-D reactor on Earth is an ideal reactor, although it also produces tritium and ns, their production rate are not so high. In this paper, a functional krF D-D laser fusion reactor in the low temperature region controlled through solid capsule injection ^{11}B is proposed for the first time, its main fuel is deuterium and boron is an additional fuel. To increase its energy gain, we use fast ignition by injecting high-energy deuteron beams.

In a deuterium-boron (D-B) fusion reactor, approximately 43-63% of fusion energy (depending on nuclear burnup conditions) is released as charged particle energy. The high energy protons produced by side reactions of D-D and D$-^3$He fusion cause additional power through p^{11}B reaction. The $^{11}\mathrm{B} + \mathrm{p} \rightarrow 3\alpha + 8.7\mathrm{MeV}$ fusion reaction is considered a possible fuel for future fusion reactors. Its advantages over more conventional approaches (such as D-T andD$-^3$He) are the availability of materials, the absence of high-energy ns, and the ease of conversion to electrical energy. The production of this reaction is possible through magnetically confined plasma [1] and laser produced plasma [2, 3]. Although the optimal cross-section for this reaction occurs at a very high collision energy between nuclei, but free electrons that cause changes in the overlapping of nuclei may lead to an increase in the reaction rate [13]. In a D-B reactor, high-energy particles (p and^{3}He) produced by D-D and D$-^3$He reactions need to be well confined. Bremsstrahlung radiation losses with an atomic number $Z_B = 5$ related to the injection of ^{11}B increased, which reduces the heating load of the conductor and the heating of the blanket surface to convert into electricity. Therefore, in the next parts of this article, at first, the production method of the deuteron beam will be presented.

Then we write the coupled point nonlinear kinetic equations governing the fusion reactor containing D-D fuel to which solid boron has been added and taking into account the side reactions, and under available conditions, we numerically solve these equations with Maple programming. We calculate the density of fusion particles, production particles, energy, and pure fusion gain as a function of temperature and time. After that, we will compare the obtained results with the case where additional solid boron is not injected. Finally, we will discuss the significant increase in access to the fusion gain by injecting the deuteron beam and taking into account the resulting bonus energy gain.

2. Deuteron beam production mechanism

Based on the p acceleration experiments, it is suggested that the parameters of the laser and the converter plate can be adjusted to obtain ion beams in the optimal range of primary energies and spectra with low $\Delta E/E$ to use deuteron beams for fast ignition [14]. This opens the way to pay attention to fast ignition through the deuteron beam. To achieve the production of a large flux from the deuteron beam, the ponderomotive acceleration of deuterons and tritons in the supercritical plasma, which is formed by the interaction of the laser with the target, has been calculated [15]. Since the converter plate method overcomes the effects of diffusion instability in direct corona interaction [16], for this reason, we focus here on the use of the converter plate method.

Deuteron ion beam production can be done with a petawatt laser like the converter plate used in the p ignition method. Ps are usually obtained from a hydrogen coating on the surface of the converter plate. Therefore, a deuterium coating can be used to produce a deuteron beam. The main issue in discussing the use of deuteron beams in the fast ignition method is the appropriate effect of laser interaction with a plate containing a very high density of deuterons. Deuterium with a very high density has been observed in a thin metal film, such as palladium, after electrochemical loading-unloading H/D [17, 18]. During loading, the metal matrix expands significantly due to H/D placement in the intermediate spaces. When hydrogen is physically absorbed, the lattice constant of palladium increases and then reaches 4.025A°. When the chemical bond is formed with high pressure, a number of linear matrix defects, which are called dislocations, are formed in the middle distance. The diameter of the dislocation defects is twice the Burgers vector (In materials science, the Burgers vector, is a vector, often denoted as **b**, that represents the magnitude and direction of the lattice distortion resulting from a dislocation in a crystal lattice.), and their length depends on the dimensions of the palladium film. After loading, the free hydrogens are discharged to the metal film using a positive current, so that the formed cluster materials remain in that place due to the high binding energy.

Additional dislocations and clusters are formed based on loading repetition. Therefore, the process of elec-

tric loading and unloading is created repeatedly to distribute the frequent dislocation rings uniformly. After 6-10 cycles, the accumulation fraction of the clusters is saturated. Due to the need for fast ignition, the number of 10^{18} ions/cm^2 is achievable for approximately 1mm^2 thin ion target area. If the packing fraction of the cluster in the foil exceeds 0.10 in 10 nm palladium plates, the smaller accumulation fraction in the palladium plate can be compensated by using a thicker plate. But the maximum thickness is limited by the mean free path of D accelerated in the plane. Therefore, unlike the p flow source, the present cluster type plates seem to be able to provide the required flux threshold for fast ignition. Therefore, this packing fraction can be intrinsically increased by the applications of advanced nanomaterials [18]. In related but slightly different conditions, Badiei et al., found ultra-dense deuterium on the surface of iron oxide [19].

3. Comparison of KrF and ArF lasers in laser fusion

The krypton fluoride (KrF) laser utilizes the chemical properties of krypton gas and the strong oxidation power of fluorine gas to produce a laser between the two by exciting the input of strong electron energy. KrF laser has been of interest in the nuclear fusion energy research community in inertial confinement experiments. This laser has high beam uniformity, short wavelength, and the ability to change spot size to track an exploding target. The pulse width of KrF lasers in commercial applications is usually 20-30 ns [20]. This laser also uses generated plasma by short pulses of this laser light to produce soft X-ray radiation argon fluoride (ArF) is currently the shortest wavelength laser [**?**], which can be used for high gain inertial fusion due to the energy and power required.

Superior coupling of the target with an ArF laser with deep UV light, $\lambda = 193$ nm, can enable higher gains for the target through inertial confinement at much lower laser energies than previously thought [22]. The combination of deep UV light and wide bandwidth (5-10 terahertz) limits and suppresses laser plasma instabilities. Therefore, the ArF laser is a potential technology for laser fusion. It uses electron beam pumping similar to that used for large KrF amplifiers. It can also use ISI (Induced Spatial Incoherence) beam-smoothing technology, which enables highly uniform illumination of targets and provides zooming of the focal profile to track an exploding target, thus maintaining high absorption efficiency throughout the direct drive implosion. KrF technology was chosen to achieve laser fusion due to its numerous advantages. ArF laser light will in turn be superior to KrF. Laser kinetic simulations show that ArF has a 1.5 times higher intrinsic laser efficiency than KrF. These advantages can enable the development of medium-sized and low-cost inertial fusion power plant units that operate with laser energies much lower than 1 MJ [23].

While the structure of KrF and ArF lasers are similar in many ways, there are three main differences between KrF and ArF laser amplifiers: (i) An ArF gas mixture has a lower stopping power than a traditional KrF gas mixture. Ar has about half the stopping power of Kr. For a given ArF laser aperture and pressure, it is necessary to use a lower voltage and higher current electron beam to achieve a given deposition rate. (ii) At a given electron beam pump rate, ArF has a lower gain than KrF, but ArF has a higher saturation current. (iii) There is much less absorption by F_2 at 193 nm than at 248 nm. The anticipated net effect of the above is that ArF can be significantly more efficient than KrF. Therefore, in this work, we have used an ArF laser to fuse the target capsule. The key components of an electron beam pumped excimer laser are shown in Figure 1.

The system of equations that are used to describe the incoherent amplification of laser pulses in ArF media is of the form [24]:

$$\frac{dN_l}{dt} = -\frac{N_l - \Theta N_b}{\tau_\upsilon} - \frac{\Theta_c N_l - \Theta_b N_k}{\tau_{bc}} - \frac{N_l}{\tau_l} - \sigma N_l I \quad (1)$$

$$\frac{dN_k}{dt} = -\frac{N_k - \Theta N_c}{\tau_\upsilon} - \frac{\Theta_b N_k - \Theta_c N_c}{\tau_{bc}} - \frac{N_k}{\tau_k} \quad (2)$$

$$\frac{dN_b}{dt} = \alpha R - \frac{\Theta_c N_b - \Theta_b N_c}{\tau_\upsilon} - \frac{N_b}{\tau_b} - \sigma N_l I \quad (3)$$

$$\frac{dN_c}{dt} = \beta R - \frac{\Theta_b N_c - \Theta_c N_b}{\tau_\upsilon} - \frac{N_c}{\tau_c} \quad (4)$$

$$\frac{\partial I}{\partial x} + \frac{1}{c}\frac{\partial I}{\partial t} = (\sigma N_l - \rho) I \quad (5)$$

Where $N_l = \sum_{v=0}^{1} N_{cv}$ and $N_k = \sum_{v=0}^{1} N_{cv}$ are the sums of a population of the laser levels in the b-state and corresponding levels in the c-state (the population of the l and k state respectively); τ_v is the vibrational relaxation time for the L and K state; $\Theta = \sum_{v=0}^{1} \Theta_v$; τ_L and τ_k are the decay time of the l and k state, respectively [24].

An exact description of the generation process in the excimer laser requires Eqs. (1-5) to be solved simultaneously with the equations describing the kinetics of formation and quenching of excimer molecules. In particular, it enables the determination of the dynamics of collisional relaxation times and absorptive losses of the medium and the determination of the exact form of the $R(t)$ function. Because, in the analyzed case of short pulse generation, the actual form of the $R(t)$ function is of secondary importance and the changes in relaxation times and losses can be accepted

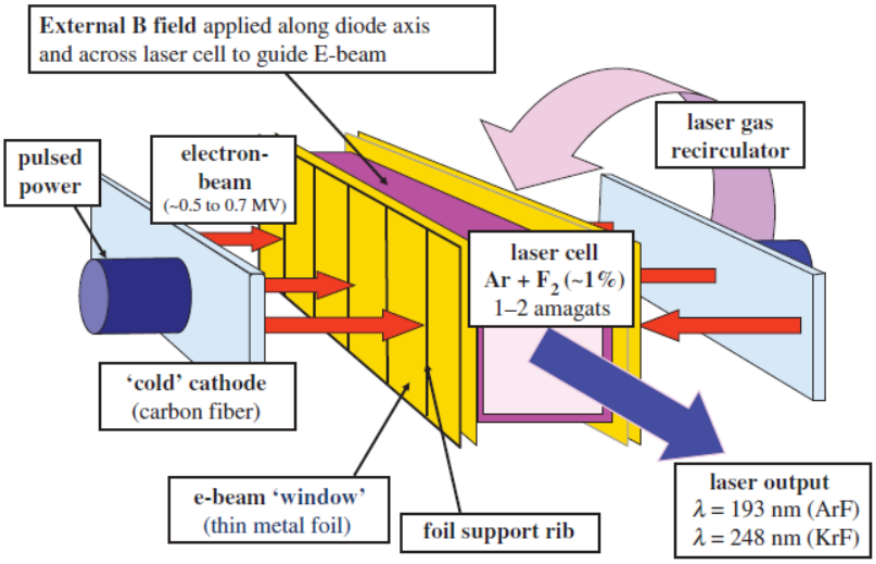

Figure 1: Schematic of the components of an excimer laser amplifier pumped with an electron beam, including pulse power, cathode, electron beam window, laser cell, and external magnetic field to guide the electron beam into the gas cell. A laser gas circulator can cool the laser gas and enable a high repetition rate pulse operation.

as slow, it was assumed in the model that the $R(t)$ function is given and relaxation times and medium losses are fixed. The $R(t)$ function was assumed in the form $R(t) = R_0 \exp\left[-(t/T_p)^4\right]$,where T_p is pulse duration. While the numerical values of the medium parameters were taken for ArF laser, from [25, 27].

In our model, as the accessible vibrational levels of the ArF*(B) state, we took the levels $v = 0, 1$. Their calculation showed that the vibrational populations in $v = 0, 1$ can all be added efficiently. However, the vibrational quantum number dependence on its accessibility makes the model complex, and also the consideration of their gain spectrum widths is necessary. Therefore, for simplicity, we ignored the contribution of higher vibrational, because the quantity of characteristic time constant of τ_v depends on the vibrational quantum number considered, the τ_v obtained in this paper is only valid for the model with the access levels of $v = 0, 1$. The quantities of Θ_b, Θ_c, and Θ are calculated by the energy gaps of $E_b - E_c = 80\ \mathrm{cm}^{-1}$ and $\Delta E_v = 327\ \mathrm{cm}^{-1}$ and the instantaneous gas temperature.

By numerical solving equations 1-5 using MATLAB programing, the population of levels B and C as well as their vibrational levels were calculated, which is shown in Figure 2. As presented in Fig.2, the population inversion of levels after time 5 ns reaches saturation. The gain recovery curve $g(t) = \sigma N_l(t)$ for the ArF amplifier obtained from Eqs.(1-5) at the parameters given above is presented in Fig.3. Our value for the saturation energy density equals $E_{\mathrm{sat}} = hc/\lambda\sigma = 32\mathrm{j/m}^2$ and

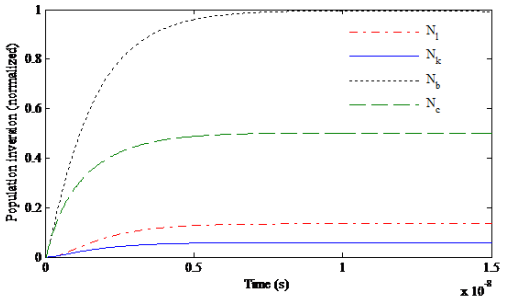

Figure 2: Population inversion of levels b, c, and the levels of vibration

for I_{sat} as shown in Fig.4 with solving Eqs.(1-5) is obtained $I_{\mathrm{sat}} = 3.2 \times 10^{14}\mathrm{W/m}^2$ and this value equals to: $I_{\mathrm{sat}} = E_{\mathrm{sat}}/\tau = hc/\lambda\sigma\tau = 3.2 \times 10^{14}\mathrm{W/m}^2$. Our amplifier system as presented in Fig.4 is routinely operated with a maximum intensity 2.2×10^{18} almost equal to 5 kJ output.

4. Introduction of widely used fusion fuels

The probability that a fusion reaction will occur depends on the cross-section where the reaction takes place. Since the deuterium-tritium fusion reaction has the largest cross-section, it is the most likely to occur. This reaction, like fission reactions, does not have radioactive waste and releases a lot of energy. Therefore, this reaction has attracted a lot of attention. Although the cross-section of the D-T reaction is much higher, the

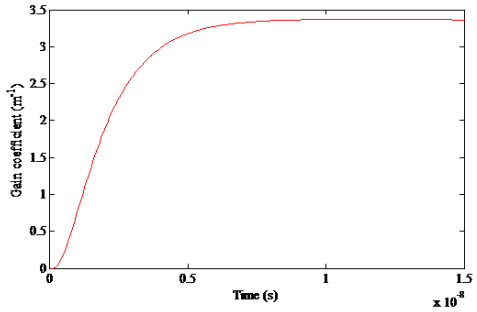

Figure 3: Gain recovery curve for ArF amplifier.

amount of tritium in nature is not high, and it is a beta emitter, and for its production, and to produce it, you need blankets containing lithium, which is expensive to make. While deuterium is a stable isotope of hydrogen. In addition, the neutron production from the deuterium-deuterium fusion reaction is much lower.

The D-D nuclear fusion reaction takes place from the following two channels with almost equal probability:

$$D + D \rightarrow T + p + 4.03MeV \quad \text{(a)}$$

$$D + D \rightarrow {}^{3}He + n + 17.59MeV \quad \text{(b)}$$

By increasing the additional solid boron to the D+D fuel capsule, the following reaction is also performed:

$${}^{11}B + p \rightarrow 3\alpha + 8.7MeV \quad \text{(c)}$$

According to these reactions, fast particles are produced and these particles deposit almost all their energy in the plasma as heat. Also, the following side reactions take place:

$$D + T \rightarrow {}^{4}He + n + 17.6\ MeV \quad \text{(d)}$$

and

$$D + {}^{3}He \rightarrow {}^{4}He + p + 18.35\ MeV \quad \text{(e)}$$

5. Particle and energy balance equations for controlled fusion

In this work, the balance equations of particle and energy are used, and in this model, the main fuel is D-D, but the solid boron is known as additional solid fuel that is injected into the main fuel. In this section, in addition to (deuterium-deuterium) reactions, we will study the behavior of (D-T), (D-^{3}He), and (p-^{11}B) reactions as side fusion reactions for the first time and then we will calculate their density and release energy as a function of temperature and time. The mentioned model for the selected different fuels is expressed by the following coupled non-linear point kinetic balance differential equations to the particle and energy [28]:

$$\frac{dn_D}{dt} = S_D - n_D\langle\sigma v\rangle_{DT}n_T + [\langle\sigma v\rangle_{DD,pT} + \langle\sigma v\rangle_{DD,n^3He}]\frac{(n_D)^2}{2} + \langle\sigma v\rangle_{D^3He}n_D n_{^3He} \quad (6)$$

$$\frac{dn_T}{dt} = \langle\sigma v\rangle_{DD,pT}\frac{(n_D)^2}{2} - \langle\sigma v\rangle_{DT}n_D n_T \quad (7)$$

$$\frac{dn_{^3He}}{dt} = \langle\sigma v\rangle_{DD,n^3He}\frac{(n_D)^2}{2} - \langle\sigma v\rangle_{D^3He}n_D n_{^3He} \quad (8)$$

$$\frac{dn_P}{dt} = \langle\sigma v\rangle_{DD,pT}\frac{(n_D)^2}{2} + \langle\sigma v\rangle_{D^3He}n_D n_{^3He} - \langle\sigma v\rangle_{pB}n_p n_B - \frac{n_P}{\tau_P} \quad (9)$$

$$\frac{dn_\alpha}{dt} = \langle\sigma v\rangle_{DT}n_D n_T + \langle\sigma v\rangle_{D^3He}n_D n_{^3He} + 3\langle\sigma v\rangle_{pB}n_P n_B - \frac{n_\alpha}{\tau_\alpha} \quad (10)$$

$$\frac{dn_B}{dt} = S_B - \langle\sigma v\rangle_{pB}n_p n_B - \frac{n_B}{\tau_B} \quad (11)$$

$$\frac{dE}{dt} = -\frac{E}{\tau_E} + P_{fusion} - P_{rad} \quad (12)$$

In the above equations,n_D, $n_{3\mathrm{He}}$, n_α, n_p, n_T, n_n, and n_B represent the particle densities of deuterium,helium-3,alpha,proton,tritium,neutron, and boron respectively. τ's and τ_E represent the confinement time of existing particles and energy, respectively. E is the net energy produced by performing the desired fusion reactions. The power of fusion is determined by the following relation:

$$P_{\mathrm{fusion}} = Q_{DT}n_D n_T\langle\sigma v\rangle_{DT} + Q_{D^3He}n_D n_{^3He}\langle\sigma v\rangle_{D3He} + Q_{p^{11}B}n_p n_{^{11}B}\langle\sigma v\rangle_{n11B} + Q_{DD}n_D^2(\frac{1}{2}\langle\sigma v\rangle_{DD,pT} + \frac{1}{2}\langle\sigma v\rangle_{DD,n^3He}) \quad (13)$$

$\langle\sigma v\rangle$'s are the reactivity of the fusion reactions mentioned above and the Q's are the released energy from these fusion reactions. $\langle\sigma v\rangle_{DD,pT}$ and $\langle\sigma v\rangle_{\mathrm{DD}n^3\mathrm{He}}$ are sigma vee parameters for reactions (a) and (b) reactions, respectively. S_D, and S_B represent the rate of injection of deuterium and boron fusion particles, respectively. P_{rad} 's are the rate of radiation energy loss due to the aforementioned fusion reactions. In this work, the dissipation radiation P_{rad} related to the desired fusion reactions is approximately expressed as follows:

$$P_{rad} = P_{brem} = A_b Z_{eff} n_e^2 \sqrt{T} \quad (14)$$

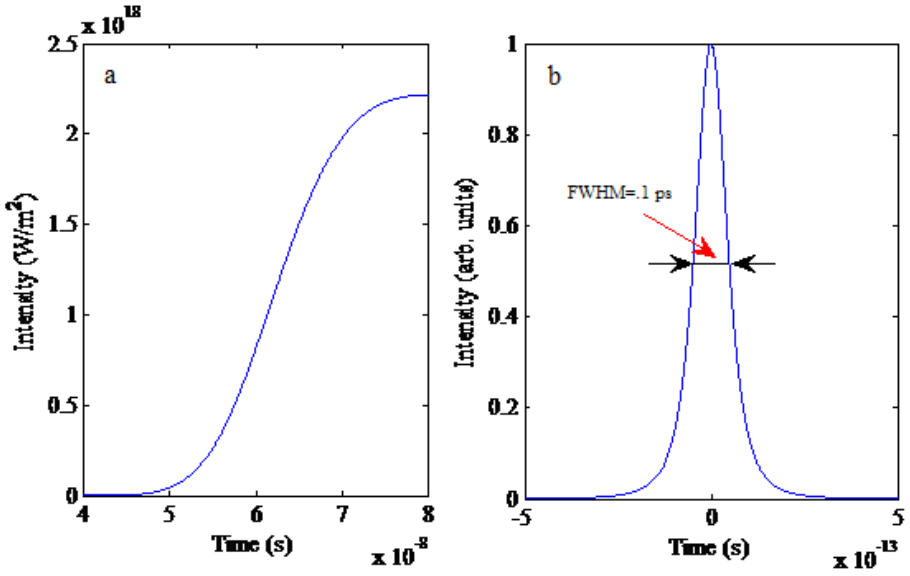

Figure 4: a: output intensity ArF laser pulse, b: Lorentzian shape of the emission spectrum of ArF laser

In the above equation, A_b is the bremsstrahlung coefficient, Z_{eff} is the effective atomic number, n_e is the electron density, n is the plasma density, and T is the plasma temperature. From the numerical solution of the above coupled point differential kinetic equations using Maple programming under selected conditions: $S_D = 4.22 \times 10^{22}\text{cm}^{-3}$ $S_B = 2.2 \times 10^{12}\text{cm}^{-3}$ $\tau = \tau_P = \tau_\alpha = \cdots = 9 \times 10^{-12}\text{s}$ $\tau_E = 1/4\tau$ and the initial condition: $n_D(0) = 4.22 \times 10^{22}\text{cm}^{-3}$ $n_B(0) = 2.2 \times 10^{12}\text{cm}^{-3}$ $E(0) = 0$ $n_\alpha(0) = 0$ $n_P(0) = 0$ $n_{3\text{He}}(0) = 0$ $n_n(0) = 0$ we obtain the time and temperature dependence of the number density of n_D, $n_{3\text{He}}$, n_α, n_p n_T, n_n, and E particles. Fusion gain can be determined from the following equation:

$$G = \frac{E}{E'} \tag{15}$$

Where E is the net energy resulting from the fusion reactions presented above and E' is the energy of the ArF laser required to start the fusion reaction. Also, in these equations, the reactivity ($\langle\sigma v\rangle$) is strongly nonlinear, positive, and a bounded function of the plasma temperature T, which is expressed by the following relations for the different fuels investigated in this work:

$$\langle\sigma v\rangle = C_1\zeta^{-5/6}\xi^2 exp\left(-3\zeta^{1/3}\xi\right) \tag{16}$$

Where

$$\zeta = 1 - \frac{C_2T + C_4T^2 + C_6T^3}{1 + C_3T + C_5T^2 + C_7T^3} \tag{17a}$$

and

$$\xi = \frac{C_0}{T^{\frac{1}{3}}} \tag{17b}$$

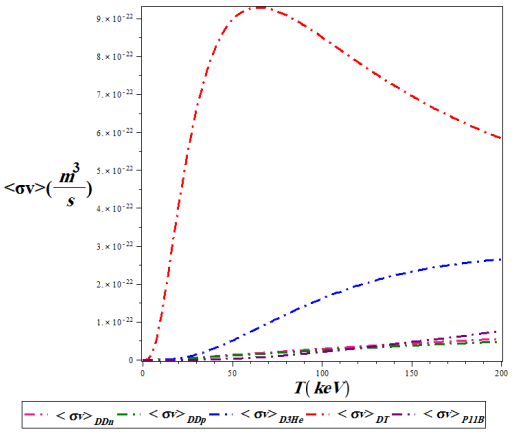

Figure 5: Variations of reactivity for different fusion reactions as a function of temperature

The parameter C_i is found in [29] for fusion reactions (a) to (e).

6. Findings and discussion

In Figure5, we draw the temperature dependence diagram of the reactivity of fusion reactions (D-T), (D-D), (D-^{3}He), and (p-^{11}B) according to equations (16) and (17) in the temperature range of 1 to 200 keV. As can be seen, the D-T fusion reaction has the highest fusion gain in this temperature range.

Also in Figure 6, with solving of the coupled nonlinear equations (6) to (12) under the presented conditions as a function of temperature and time, the density of fusion particles and production particles and fusion

energy, and then the net gain resulting from the fusion of D-D fuel with consideration of the side reactions $D + T$, $D + {}^3He$ and ${}^{11}B + p$ are given for two cases i) with and ii) without additional boron solid injection.

It can be seen from the comparison of the graphs in Figures 6-(a) and (b), that the density of deuterons, either with or without additional injection of the solid boron decreases with increasing time and finally reaches the characteristic value of the steady state. Temperature does not significantly affect the density of deuterons consumed with time. It can be seen from diagrams 6-((c) and (d)), ((e) and (f)), ((g) and (h)), ((i) and (j)), ((k) and (l)), ((m) and (n)), and ((o) and (p)) that over time for both cases with and without additional solid injection, with increasing time, the number of alpha particles, neutrons, tritium, helium-3, protons, fusion energy and finally the energy gain increases and then decreases. Because in the beginning, the amount of the mentioned fusion reactions is low, with the time spent, the number of these reactions increases until they reach their maximum value. Then, because the amount of fusing fuels is reduced due to their consumption, the graphs start a downward trend and finally reach the characteristic of the steady state. It should be noted that the mentioned quantities increase with increasing temperature because the rate of reactivity increases. It can be seen from Figure 6-(q) that because the injected additional solid boron is consumed during the fusion reactions, its amount decreases until it finally reaches the characteristic value of the steady state. Temperature variations have no significant effect on its density.

It is important to mention that the maximum energy gain in the state without additional solid injection is about 6.7 at a temperature of 100 keV. While energy gain maximum due to additional solid boron injection to D-D fuel increases nearly ten times and reaches approximately 70 at the same temperature. In other words, we conclude that by injecting the additional solid boron into the D-D fuel capsule, the energy from fusion and subsequently the fusion gain increases significantly, because the additional solid boron helps to perform $P^{11}B$ reactions.

7. Determining the stopping power and gain of the bonus energy resulting from the addition of solid boron to the spherical D-D fuel capsule with simultaneous injecting of a deuteron beam in fast ignition using an ArF laser

According to Figure 7, the fuel capsule with a uniform density of 300 $g.cm^{-3}$ is considered. It is assumed that the deuterons are produced instantaneously and collide with the fuel in a cone-guided manner and create a hot spot with a radius of $20\mu m$. Also, the electrons and background ions in the plasma are at the same temperature and the number of ions in the pre-condensed fuel is equal to the number of background electrons.

The contribution of stopping deuterons in D-D fuel plasma is given by [30]:

$$\frac{dE^{D/d}}{dx} = -\frac{2\pi e^4 n_d}{E_D}\left\{\left(-\frac{4}{\sqrt{\pi}}\sqrt{x^{D/d}}e^{-x^{D/d}} + \mathrm{erf}\left(\sqrt{x^{D/d}}\right)\right)\ln\Lambda_{D-d} + \mathrm{erf}\left(\sqrt{x^{D/d}}\right) + \ln\left(1.123\sqrt{x^{D/d}}\right)\right\} \tag{18}$$

In the above equations, e is the unit charge, n_d is the numerical density of deuterons, in the D-D fuel, and E_D is the kinetic energy of the deuteron, $\mathrm{erf}(x) = 2/\sqrt{\pi}\int_0^x \exp\left(-t^2\right) dt$ is the error function. Also, $x^{D/d} = E_D/T$, and the expression $\ln(1.123\sqrt{x^{D/d}})$ express the contribution of the collective effect, T is the fuel temperature and $\ln\Lambda_{D-d}$ represents the Coulomb logarithm of the deuteron-deuteron interaction, whose formula is given by:

$$\ln\ \Lambda_{D-d} = \ln\frac{\sqrt{T_d/4\pi e^2 n_d}}{e^2/(E_D + T_d)} \tag{19}$$

In Figure 8, we have drawn the 3D variations of the Coulomb logarithm of the interaction of deuterons with deuterons versus deuteron energy at different temperatures related to D-D fuel with a density of $300 g.cm^{-3}$. Deuterons create a bonus energy gain as they slow down while fusing with fuel ions. Depending on the conditions of the target plasma, this added energy gain can have a significant contribution. This added energy increases the total energy gain of the system. The value of G as the energy gain, the ratio of the total fusion energy produced E_f through the beam-target interactions to the input energy of the ion injected into the plasma E_I, is defined as follows [31]:

$$G_{D+D} = n_D\frac{\int_{E_{th}}^{E_I} S\,(E)\,dE}{E_I} \tag{20}$$

In this relation, E_{th} and E_I are the average energy of the background plasma ($E_{th}=2k_BT$) and the initial energy of the injected ion, respectively.

$\int_{E_{th}}^{E_I} S\,(E)\,dE$, is the fusion production energy caused by ns and charged particles. S (E) is the fusion probability of an ion with energy E, which slows down with the amount of dE. This probability is calculated through the following equation [32, 34]:

$$S\,(E) = \sum_k K_k[<\sigma V(E)>_k]_{Ik}(E_f)_{Ik}/dE/dt \tag{21}$$

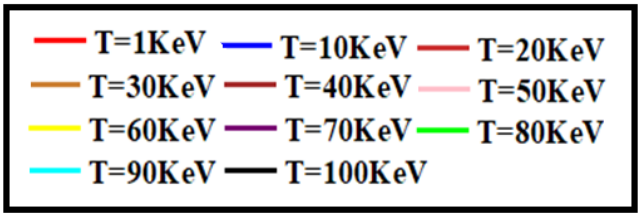

The range of colors corresponding to the selected temperatures

With solid boron injection to D-D fuel

Without solid boron injection to D-D fuel

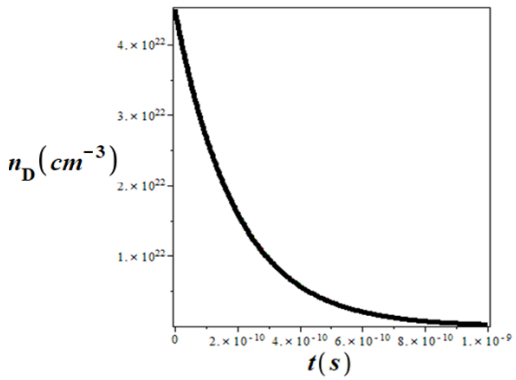

(a)

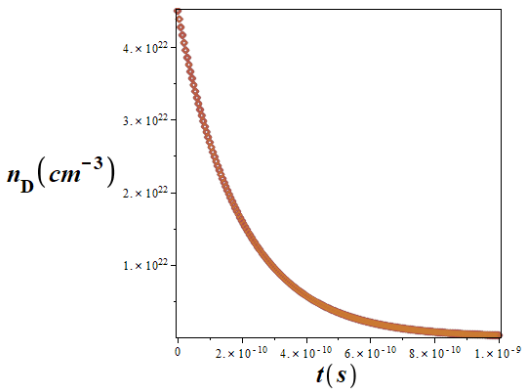

(b)

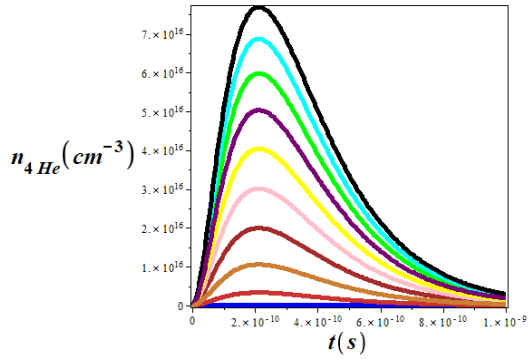

(c)

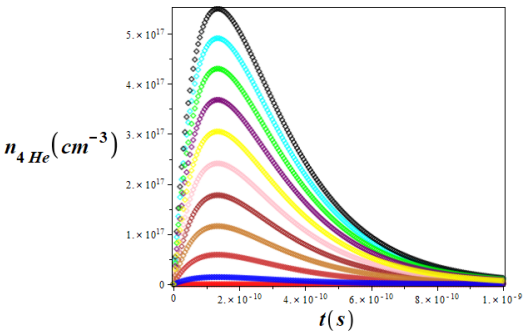

(d)

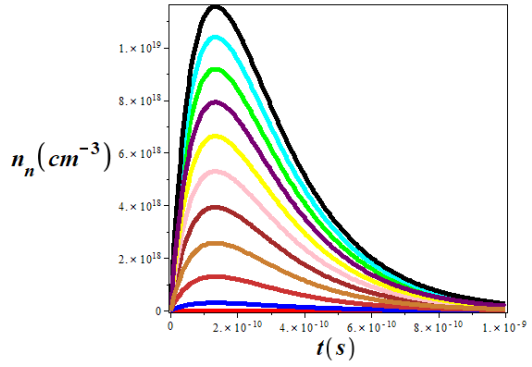

(e)

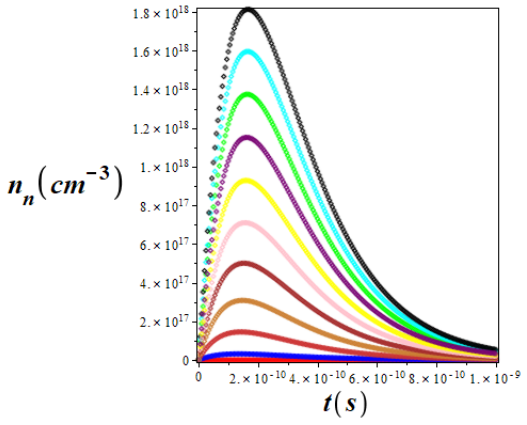

(f)

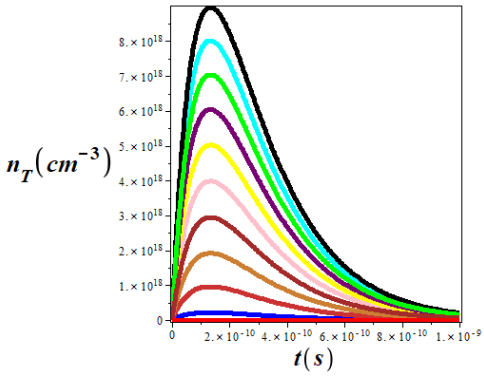
$n_T(cm^{-3})$
$t(s)$

(g)

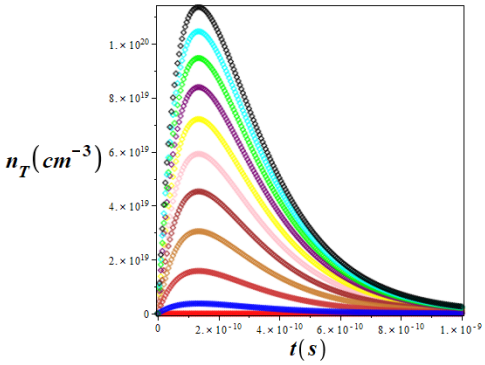
$n_T(cm^{-3})$
$t(s)$

(h)

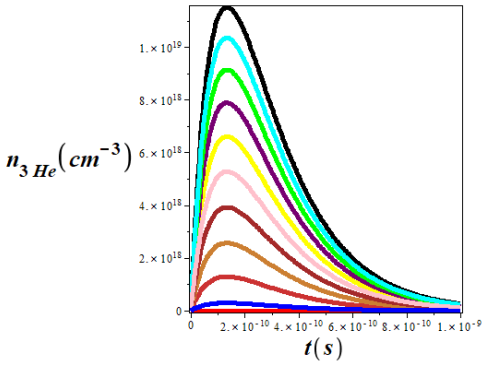
$n_{3\,He}(cm^{-3})$
$t(s)$

(i)

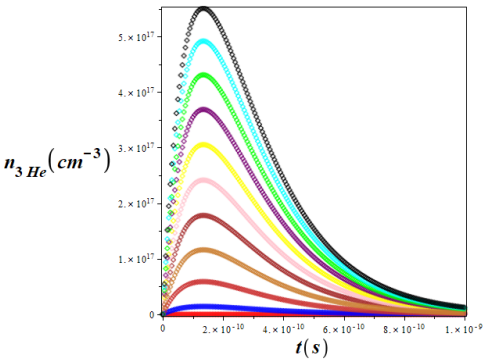
$n_{3\,He}(cm^{-3})$
$t(s)$

(j)

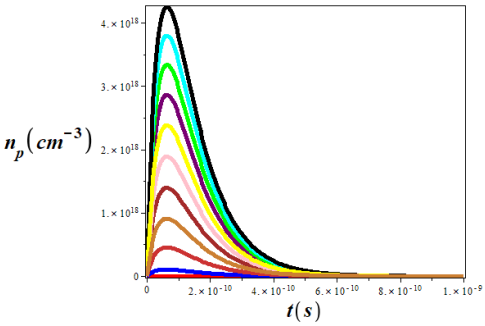
$n_p(cm^{-3})$
$t(s)$

(k)

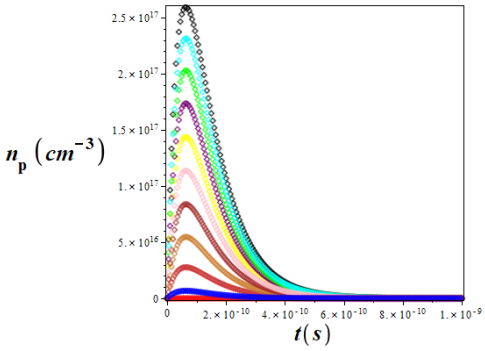
$n_p(cm^{-3})$
$t(s)$

(l)

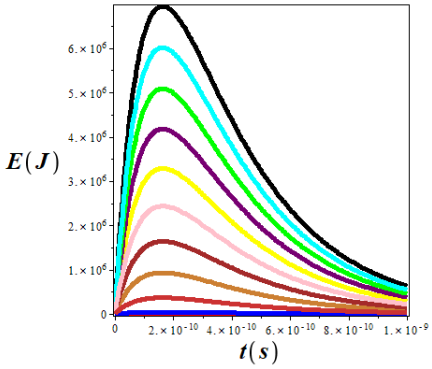
$E(J)$
$t(s)$

(m)

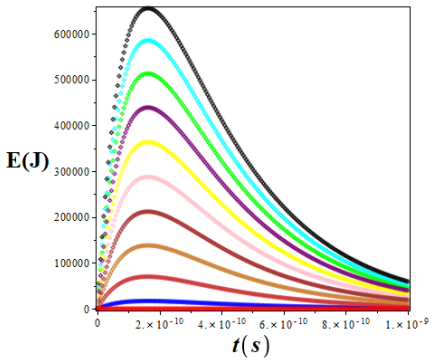
E(J)
$t(s)$

(n)

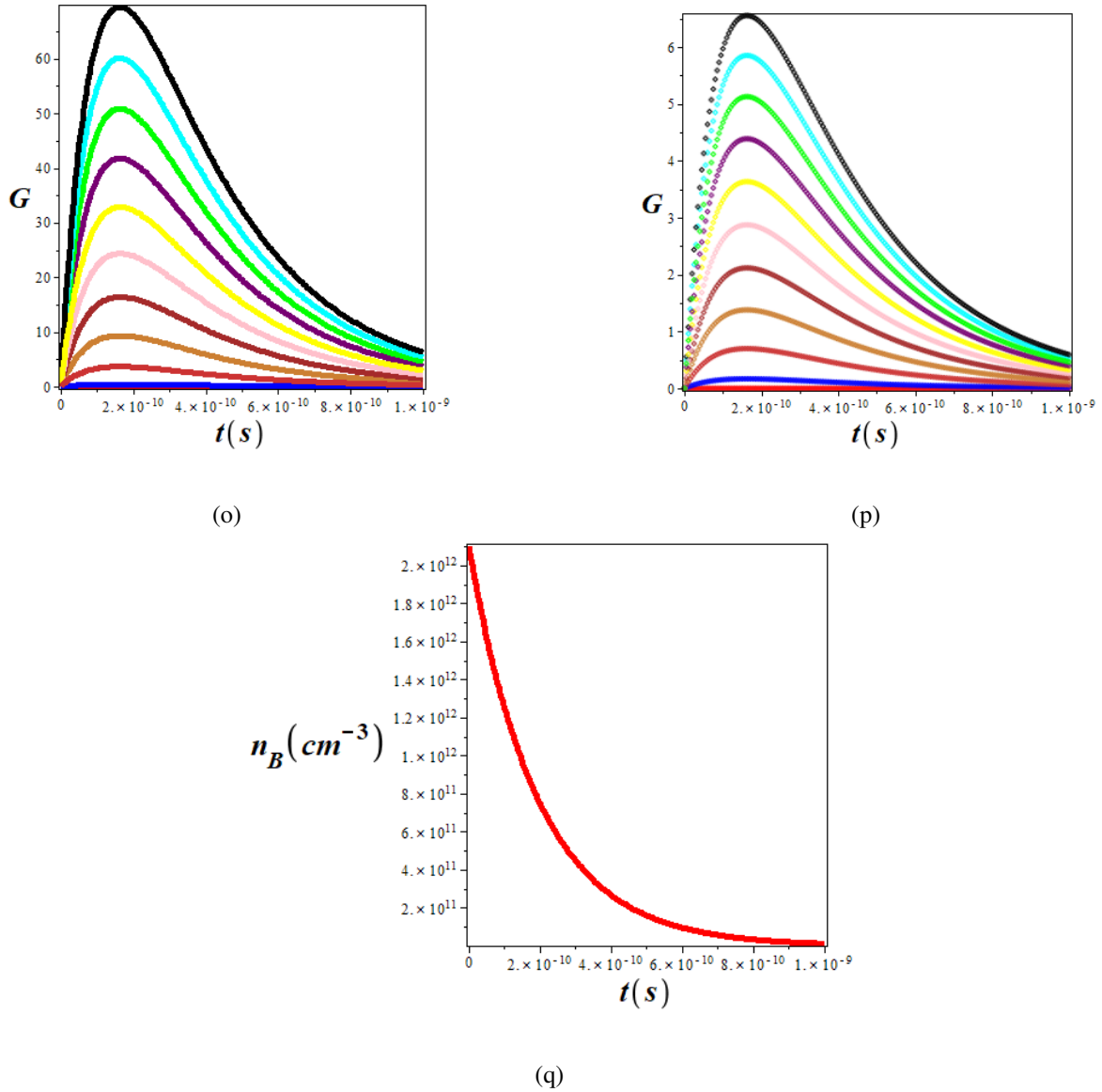

Figure 6: 2D time variations of the density of consumed((a),(b) and(q)), produced particles((c),(d),(e),(f),(g),(h),(i),(j),(k)and(l)), energy((m)and(n)), and gain((o)and(p)) of fusion resulting from the D-D fusion reaction and the density of additional injected boron into the fuel capsule with taking into account the side reactions of fusion D + T, D + ^{3}He and ^{11}B + p with and without additional boron solid injection at different temperatures.

dE/dt is the time rate of energy loss of the injected ion, which is defined as follows for D-D pre-compressed fuel (ignoring energy dispersion of injected ions during slowing down):

$$\frac{1}{n_D}\left(\frac{dE}{dt}\right)_{\mathrm{D+D}} = \frac{Z_I^2 e^4 m_e^{1/2} E \ln \Lambda_{D+d}}{3\pi(2\pi)^{1/2}\varepsilon_0^2 m_I (k_B T_e)^{3/2}} \times \left[1 + \frac{3\sqrt{\pi} m_I^{3/2}(k_B T_e)^{3/2}}{4 m_k m_e^{1/2} E^{3/2}}\right] \quad (22)$$

Where m_e is the mass of the electron and m_i is the mass of the ion and both of them are in terms of atomic mass units.

Figure 9 shows that dE/dtdecreases with increasing electron temperature and deuteron energy.$<\sigma V>_{Ik}$, is the reactivity of fusion for I ion injected with the index k, which has the atomic fraction K_k in the target. $(E_f)_{Ik}$, is the energy released in a fusion and T_e is the target electron temperature. $(E_f)_{Ik}$, is carried by particles produced by fusion reactions such as fast ns and charged particles. But for heating the hot spot, the surface density ρr (r and ρ are the radius and density of the hot spot, respectively) of the hot spot is too small

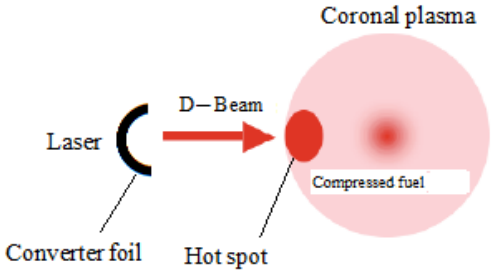

Figure 7: Scheme of fast ignition of D-D fuel using deuteron beam injection

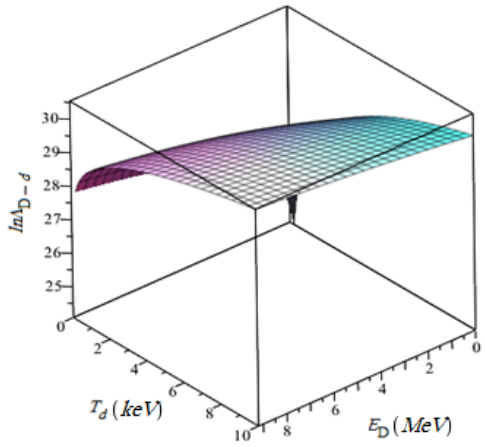

Figure 8: 3D variations of Coulomb logarithm of the interaction of deuterons with deuterons in terms of deuteron energy at different temperatures related to D-D fuel with a density of 300g.cm^{-3}

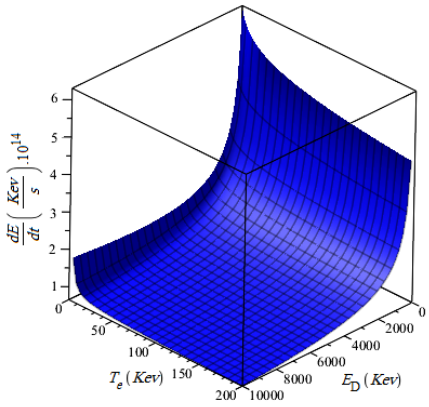

Figure 9: 3D variations of dE/dt in terms of electron temperature and deuteron energy in pre-compressed D-D fuel with a density of 300g.cm^{-3}

to significantly slow down the ns, so only charged particles are involved in this. For the D-D reaction, approximately 63% of the total energy is useful. To avoid mistakes, we introduce a new factor Q to show energy multiplication to heat the hot spot by charged particles. Therefore, the bonus energy percentage due to D-D fusion isQ_{D+D}= 63%G_{D+D}, which is related to D-D precompressed fuel as a result of the D-D fusion reaction.

Therefore, the total energy that can be deposited inside the target is equal to the sum of the deuteron energy and the energy of the charged particles produced by the deuteron-target fusion (bonus energy):

$$E_{tot} = E_D(1 + Q) \tag{23}$$

As can be seen E_D, and Q parameters play an important role in the bonus energy and the total energy deposited by the deuteron beam. It should be noted that $E_{tot}$is the total deposited energy by the ion beam plus the beam-target fusion contribution in the hot spot. It is not equal to the total energy entering the target which is often mentioned in energy studies.

In Figure 10, the variations of Q_{D+D} (bonus energy due to D-D fusion) and E_{D+D} in terms of deuteron energy at different electron temperatures in the pre-compressed D-D fuel containing additional solid boron with a density of 300g.cm^{-3} are shown. As can be seen from these figures, $Q_{D+D}$and E_{D+D} are functions of the electron temperature and the energy of the injected deuteron beam, such that with an increase of electron temperature and injected deuteron beam energy, these quantities increase non-linearly and almost linearly, respectively.

Tables 1 and 2 respectively show the percentage of bonus energy and total deposited energy (sum of deuteron and bonus energy) in the average initial deuteron energy and different hot spot temperatures in pre-compressed D-D fuel containing additional solid boron. As it is known, in this fuel, the percentage of bonus energy and total deposited energy is higher in smaller E_D and higherT_e. In other words, E_{tot} has a significant increase compared to the case without deuteron beam injection when T_e is larger and E_D is smaller.

From the comparison of the numbers in Tables 3A and B, it can be seen that by injecting a deuteron beam and depositing the resulting bonus energy in the desired fusion fuel capsule for two modes without and with additional solid boron injection into the desired fuel capsule, the energy gain related to the additional solid boron injection mode shows a significant increase compared to the mode without additional solid mode injection. The importance of these estimates is shown through the following example for D-D pre-compressed fuel containing additional solid boron.

Table 1: Bonus energy percentage (Q_{DD}) for the initial average energies of the injection deuteron beam (1, 2, 3, and 10 MeV) in the hot spot temperature range of $5 \leq T(\text{keV}) \leq 70$ in the pre-compressed D-D fuel containing additional solid boron with a density of 300g.cm^{-3}

Hot spot temperature in DD fuel					
70 keV	40 keV	10 keV	5keV		
5.6	2.8	0.8	0.1	1MeV	The average initial energy of injection deuteron beam
5.8	3.8	1.2	0.2	2MeV	
5.2	3.9	1.3	0.4	3MeV	
2.8	2.4	1.2	0.5	10MeV	

Table 2: The total deposited energy E_{D+D} (in MeV) for the initial average energies of the injected deuteron beam(1, 2, 3, and 10 MeV)in the hot spot temperature range $5 \leq T(\text{keV}) \leq 70$ in D-D pre-compressed fuel containing additional solid boron with a density of 300g.cm^{-3}

Hot spot temperature in DD fuel					
70keV	40keV	10keV	5keV		
1.01	0.82	0.74	0.63	1MeV	The average initial energy of injection deuteron beam
2.28	2.18	2.04	2.02	2MeV	
3.24	3.15	3.03	3.03	3MeV	
10.19	10.18	10.17	10.1	10MeV	

For example, it is assumed that the ion energy of 10kJ (6.24×10^{16} MeV) is required to be deposited inside the hot spot [35, 36, 37]. So that the average energy of each deuteron is considered to be approximately 2 MeV.

In this case, a total number of 3.12 x 10^{16} deuterons from the converter plate is required without considering the additional deposited energy by deuteron-target beam fusion. According to Table 2, the actual deposited energy in the pre-compressed D-D fuel containing additional solid boron for E_D= 2MeV varies from 2.00 to 2.04 at different T_e (1 to 10 keV). If the average of 2.02 MeV is used as the actual deposited energy for each deuteron, then the actual number of deuterons required is $6.24\times\frac{10^{16}}{2.02}= 3.09\times10^{16}$, so that the number of required ions decreases by 10%. This is an important advantage because all ion acceleration designs consider the efficiency of the converter plate as a determining factor.

8. Conclusion

There are various candidates for fusion plasmas in the core of reactors, which are called advanced plasmas. The number of neutrons produced in them is much less compared to D-T fusion and therefore they do not have the problems related to radioactivity, safety, and the environment. To solve these problems, studies have been done to find plasmas that can replace the D-T plasma cycle. Among the aneutronic fuels for these plasmas are $P^{11}B$. The cycle of these fuels produces a much smaller number of ns than the D-T fuel cycle, and the energy of these produced ns is also much less. Therefore, the rate of destruction of materials will decrease.

Our studies in this article have shown that the D-D plasma cycle along with additional solid boron injection causes the creation of protons and the fusion reactions caused by the protons produced with the injected ^{11}B, which significantly solves the problem of the life of the reactor components by reducing neutron destruction. Secondly, it is important from this point of view that the maximum energy gain in the state without additional solid boron injection is about 6.7 at a temperature of 100 keV. While the maximum energy gain as a result of additional solid boron injection to D-D fuel has increased nearly ten times and reached a value of about 70 at the same temperature. Also, our previous calculations show that the fusion gain of the D-T reaction with deuteron beam radiation gives the maximum fusion gain of this reaction occurs at the resonance temperature of 70 keV and is about 20 (see Table 3 in Ref. [37]). Now if we compare this value with the highest gain obtained from D-D fusion with simultaneous deuteron beam radiation by adding solid boron, we find that in this work, the gain has increased by about 50 units, which makes the role of adding external solid boron very important.

In other words, we conclude that by injecting additional solid boron into the D-D fuel capsule, the energy from fusion and subsequently the fusion gain will increase significantly. Also, the injected deuteron beam deuterons create a bonus energy gain as they slow down

Table 3: The maximum of the total produced energy gain, including the total deposited energyE_{D+D} for the initial average energies of the injected deuteron beam (1, 2, 3, and 10 MeV) in the hot spot temperature range of 5≤T(keV)≤70 in D-D pre-compressed fuel a) without b) with additional solid injection

a)

Hot spot temperature in DD fuel					
70keV	40keV	10keV	5keV		
5.51	2.82	0.94	0.73	1MeV	The average initial energy of injection deuteron beam
6.78	4.18	2.24	2.12	2MeV	
7.54	5.15	3.23	3.13	3MeV	
14.69	12.18	10.37	10.2	10MeV	

b)

Hot spot temperature in DD fuel					
70keV	40keV	10keV	5keV		
43.01	16.82	2.74	1.73	1MeV	The average initial energy of injection deuteron beam
44.28	18.18	4.04	3.12	2MeV	
45.24	19.15	5.03	4.13	3MeV	
52.19	26.18	12.17	11.2	10MeV	

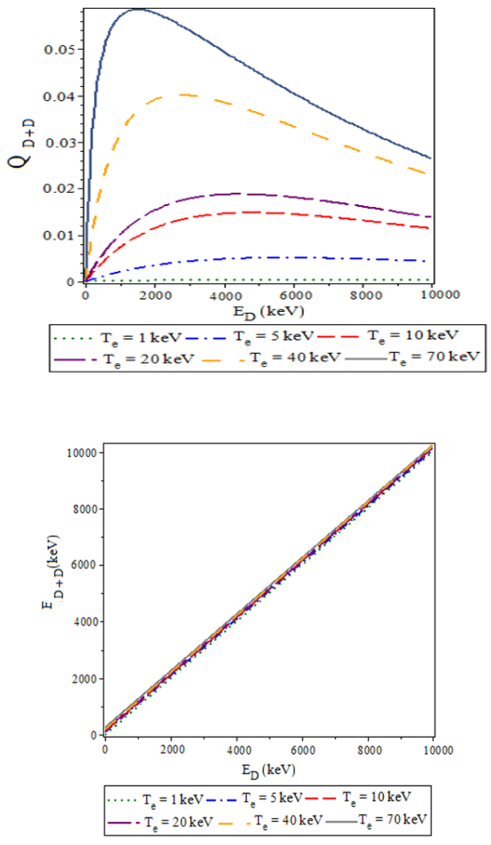

Figure 10: Variations of a) Q_{D+D} and b) E_{D+D} in terms of deuteron energy at different electron temperatures in D-D pre-compressed fuel containing additional solid boron with a density of 300g.cm^{-3}

during fusion with the fuel ions. This added energy increases the total energy benefit of the system. Parameters E_D (initial beam energy) and Q (energy multiplication factor) play an important role in the bonus energy and the total deposited energy by the deuteron beam in the D-D fuel containing additional solids. Q_{DD} value for E_D300keV decreases with increasing E_D and increases in all cases with increasing T_e. While the amount of total deposited energy in constant E_D increases withT_e. This is one of the advantages of fast ignition using a deuteron beam, such that in smaller E_D and higherT_e, the bonus energy and the total deposited energy are higher.

Acknowledgement

This work is supported by the Islamic Azad University of Shiraz.

References

[1] M J Edwards, *Phys. Plasmas* **20**, 070501 (2013).
[2] O A Hurricane *et al., J. Nature* **506**, 7488 (2014).
[3] S Le Pape *et al., Phys. Rev. Lett.* **120**, 245003 (2018).
[4] J D Kilkenny, *Plasma Phys. and Controlled Nuclear Fusion Research* **3**, 133 (1993).
[5] M Tabak *et al., Phys. Plasmas* **1**, 1626 (1994).
[6] S P Regan, *Phys. Rev. Lett.* **111**, 045001 (2013).
[7] U Teubner *et al., Phys. Rev. E.* **54**, 4167 (1996).
[8] M Temporal, *Phys. Plasmas* **13**, 122704 (2006).
[9] M Temporal *et al., Phys. Plasmas* **15**, 052702 (2008).
[10] V T Tikhonchuk *et al., Nuclear Fusion* **50**, 045003 (2010).
[11] S Le Pape, *Phys. Rev. Lett.* **120**, 245003 (2018).
[12] L B Hopkins, *Plasma Phys. Control Fusion* **61**, 014023 (2019).
[13] R S Craxton *et al., Phys. Plasmas* **22**, 110501 (2015).
[14] H Schwoerer *et al., Nature London* **439**, 445 (2006).
[15] N Naumova *et al., Phys. Rev. Lett.* **102**, 025002 (2009).
[16] F K Azadboni, *Chinese J. Phys.* 71, 375 (2021).

[17] A G Lipson *et al., Phys. Lett. A.* **339**, 414 (2005).
[18] G H Miley *et al., J. Phys. Conference Series* **4**, 032036 (2010).
[19] S Badiei *et al., Int. J. Mass Spectrometry* **282**, 70 (2009).
[20] V Zvorykin *et al., Appl. Opt.* **59**, A198 (2020).
[21] M Azumi and E Nakahata, *SPIE* **9632**, 199 (2015).
[22] M F Wolford *et al., HEDP* **36**, 100801 (2020).
[23] M Myers *et al., PPPS* 1 (2019).
[24] F Kannari *et al., J. Appl. Phys.* **57**, 4309 (2019).
[25] J Tellinghuisen *et al., J. Chem. Phys.* **65**, 4473 (1976).
[26] J J Ewing and C A Brau, *Appl. Phys. Lett.* **27**, 350 (1975).
[27] T H Dunning and P J Hay, *Appl. Phys. Lett.* **28**, 649 (1976).
[28] S N Hoseinimotlagh *et al., Int. J. Appl. Phys. Mathe.* **4**, 93 (2014).
[29] L.M. Hively, *Nucl. Fusion* **17**, 873 (1977).
[30] C K Li and R D Petrasso, *Plasmas. Phys. Rev. Lett.* **70**, 3059 (1993).
[31] C Bathke *et al., Transactions ANS* **17**, 41(1973).
[32] D J Rose and J Clark, *Plasmas and controlled Fusion*, (MIT Press Cambridge, MA , 1965)
[33] C Bathke *et al., Transactions ANS* **17**, 41 (1973).
[34] G H Miley, *American Nuclear Society, Hinsdale, IL* (1976).
[35] S Atzeni *et al., Nuclear Fusion* **42**, L1 (2002).
[36] J C Fernandez *et al., J. Phys. Conference Series* **112**, 022051 (2008).
[37] S N Hosseinimotlagh *et al., Am. J. Energy Eng.* **2**, 65 (2014).